The Astrophysical Journal, 726:23 (11pp), 2011 January 1 doi:10.1088/0004-637X/726/1/23

SUBSTELLAR OBJECTS IN NEARBY YOUNG CLUSTERS (SONYC). II. THE BROWN DWARF POPULATION OF ρ OPHIUCHI*

Vincent Geers[1,2], Alexander Scholz[3], Ray Jayawardhana[1,6], Eve Lee[1], David Lafrenière[1,4], and Motohide Tamura[5]
[1] Department of Astronomy & Astrophysics, University of Toronto, 50 St. George Street, Toronto, ON M5S 3H4, Canada; vcgeers@astro.utoronto.ca
[2] Institute for Astronomy, ETH Zurich, Wolfgang-Pauli-strasse 27, 8093 Zurich, Switzerland
[3] School of Cosmic Physics, Dublin Institute for Advanced Studies, 31 Fitzwilliam Place, Dublin 2, Ireland
[4] Département de Physique, Université de Montréal, C. P. 6128 Succ. Centre-Ville, Montréal, QC H3C 3J7, Canada
[5] National Astronomical Observatory, Osawa 2-21-2, Mitaka, Tokyo 181, Japan
Received 2010 March 22; accepted 2010 October 25; published 2010 December 10

ABSTRACT

SONYC—Substellar Objects in Nearby Young Clusters—is a survey program to investigate the frequency and properties of brown dwarfs (BDs) down to masses below the deuterium-burning limit in nearby star-forming regions. In this second paper, we present results on the ∼1 Myr old cluster ρ Ophiuchi, combining our own deep optical- and near-infrared imaging using Subaru with photometry from the Two Micron All Sky Survey and the *Spitzer Space Telescope*. Of the candidates selected from iJK_s photometry, we have confirmed three—including a new BD with a mass close to the deuterium limit—as likely cluster members through low-resolution infrared spectroscopy. We also identify 27 substellar candidates with mid-infrared excess consistent with disk emission, of which 16 are new and 11 are previously spectroscopically confirmed BDs. The high and variable extinction makes it difficult to obtain the complete substellar population in this region. However, current data suggest that its ratio of low-mass stars to BDs is similar to those reported for several other clusters, though higher than what was found for NGC 1333 in Scholz et al.

Key words: brown dwarfs – circumstellar matter – stars: formation – stars: low-mass

Online-only material: color figures

1. INTRODUCTION

Understanding the origin of the stellar initial mass function (IMF) is one of the major topics in astrophysics. The low-mass end of the IMF, in particular, has been subject of numerous observational and theoretical studies over the past decade (see Bonnell et al. 2007).

SONYC—Substellar Objects in Nearby Young Clusters—is an ongoing project to provide a complete census of the brown dwarf (BD) and planetary-mass object population in nearby young clusters and to establish the frequency of substellar mass objects as a function of cluster environment. The resulting catalog of substellar mass candidates will provide the basis for detailed characterization of their physical properties (disks, binarity, atmospheres, accretion, and activity). The survey makes use of extremely deep optical- and near-infrared imaging, combined with the Two Micron All Sky Survey (2MASS) and *Spitzer* photometry catalogs, and follow-up spectroscopy using 8 m class telescopes, aiming to detect the photosphere of the objects, which is an essential prerequisite for an unbiased survey. Our observations are designed to reach limiting masses of 0.003 $M_\odot$, well below the deuterium-burning limit at 0.015 $M_\odot$, and in each region, we aim to cover at least ∼1000 arcmin^2.

In our first paper (Scholz et al. 2009), we presented the survey of the NGC 1333 cluster in Perseus, which was surveyed complete down to 0.004–0.008 $M_\odot$ for A_V up to 5–10 mag. We identified 12 new substellar members in this cluster based on photometry and spectroscopy and found a tentative minimum mass cutoff to the IMF at 0.012–0.020 $M_\odot$.

In this second paper, we report on the survey of the ρ Oph star-forming cloud complex. ρ Oph is one of the closest ($d = 125 \pm 25$ pc; de Geus et al. 1989) regions of active star formation. In contrast with the first SONYC field, NGC 1333, the ρ Oph cluster is not as compact and exhibits extremely high and variable levels of extinction. The main cloud, L1688, is a dense molecular core, with visual extinction up to 50–100 mag (Wilking & Lada 1983), hosting an embedded infrared cluster of around 200 stars, inferred to have a median age of 0.3 Myr, and surrounded by multiple clusters of young stars with a median age of 2.1 Myr (Wilking et al. 2005 and references therein).

To date, a population of 17 BD candidates in ρ Oph, with spectral M6 or later, have been spectroscopically confirmed by Wilking et al. (1999), Luhman & Rieke (1999), and Cushing et al. (2000). An ISOCAM survey of very young stars in ρ Oph was presented in Bontemps et al. (2001), from which a selection of candidate BDs with disks was discussed in Natta et al. (2002). For a number of BDs, Jayawardhana et al. (2002) searched for accretion signatures with high-resolution optical spectroscopy, and Jayawardhana et al. (2003) found a disk fraction of ∼67% for ρ Oph from L'-band (3.8 μm) excess. A survey of accretion rate measurements for the full ISOCAM survey was presented in Natta et al. (2006). For a recent summary of the star formation and BD population in ρ Oph, see Wilking et al. (2008). A few BDs were found and spectroscopically confirmed at about 1° away from the center of the L1688 cloud (Jayawardhana & Ivanov 2006; Allers et al. 2007).

This paper is structured as follows. Observations and data reduction of imaging and spectroscopy are described in Section 2. The photometric selection of very low mass objects is described in Section 3, and spectroscopy is presented in Section 4. The results are discussed in Section 5, and conclusions are presented in Section 6.

* Based on data collected at Subaru Telescope, which is operated by the National Astronomical Observatory of Japan.
[6] Principal Investigator of SONYC.

2. MULTI-BAND PHOTOMETRY

2.1. Optical Imaging

We obtained optical images with the Subaru Prime Focus Camera (Suprime-Cam) wide field imager (Miyazaki et al. 2002) in the Sloan Digital Sky Survey (SDSS) i' filter on 2008 August 2, with a typical range in seeing of 0.″50–0.″60. Suprime-Cam is a mosaic camera utilizing 10 CCDs arranged in a 5×2 pattern, giving a total field of view of $34' \times 27'$, with a spatial resolution of 0.″20 pixel^{-1}. The ρ Oph cluster was observed in a single field with 15 individual exposures of 120 s in a 10-point dither pattern. In total this gives an integration time of 1800 s.

We performed image reduction separately for each individual chip, using the Suprime-Cam reduction software package *SDFRED* (Yagi et al. 2002; Ouchi et al. 2004). This includes overscan subtraction, flat-fielding, distortion correction, sky subtraction, bad pixel and AG probe masking, and finally image combination. The 2MASS point-source catalog (Cutri et al. 2003) was used as a reference for the calibration of the world coordinate system, using the *msctpeak* routine from the IRAF package *MSCRED*.[7] The typical fitting residuals were of order 0.″15.

The objects were identified using the Source Extractor (SExtractor) software package (Bertin & Arnouts 1996). We require an object to have at least 5 pixels with flux above the 3σ detection limit to be extracted. The automatic aperture fitting routine in SExtractor was used to calculate the flux of each source. We chose conservative rejection criteria to minimize the number of spurious detections in the photometry database, including the rejection of objects within 25 pixels of the edge of the image, elongated objects ($a/b > 1.2$), and saturated objects. The results from the detection and rejection algorithm were verified by visual inspection to minimize the number of spurious detections and missed point sources. The final optical catalog has 5791 objects.

The chip-to-chip zero-point offsets were derived from the median fluxes of domeflat images. The absolute zero point for the mosaic was derived from observations of the SA112 standard field, which contains SDSS secondary standards (Smith et al. 2002). These standard observations were taken at the same airmass and with the telescope defocused to avoid saturation. Four standard stars were available in this field and photometry was obtained using a fixed 30 pixel radius aperture extraction. For the i' band, we derive a mean zero point of 32.588 ± 0.076 mag and a completeness limit of 24.15 ± 0.30 mag; see Figure 1.

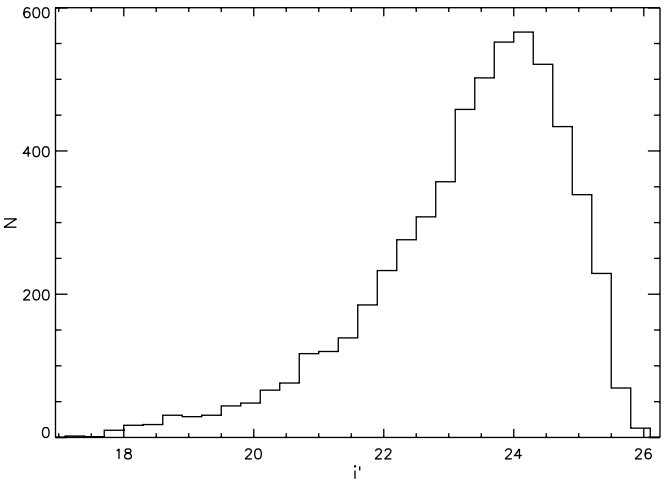

Figure 1. i'-band histogram of the objects in our photometric catalog with i'-band data. The peak at 24.15 mag indicates the completeness limit of the survey. The faintest objects in the survey are found at $i' > 26$ mag.

2.2. Near-infrared Imaging

The Multi-Object Infrared Camera and Spectrograph (MOIRCS; Suzuki et al. 2008) mounted on the Subaru telescope was used to observe ρ Oph in the J (1.26 μm) and K_s bands (2.14 μm). The data were obtained 2007 June 22–24. MOIRCS uses two detector arrays which provide a field of view of 4′ by 7′ in each pointing. We observed 24 MOIRCS fields with an overlap of 30″ between adjacent fields, encompassing the embedded subclusters ρ Oph A, B, E, and F in the L1688 cloud (Loren et al. 1990). The total imaging area coverage was 31.′5 by 26′. Each field was covered in a six-point dither pattern with individual exposure times of 100 s in J, and 50 s in K_s bands. This yields a total integration time of 600 s in the J band and 300 s in the K_s band. Significant contamination by a bright nearby source was present in 15 individual images.

The reduction was carried out with the SIMPLE-MOIRCS package.[8] First, we corrected for the offset in sensitivity between the two detector arrays. The individual frames are then flat-field corrected for flat fields and co-added by median. For the source detection we used the SExtractor, requiring at least 5 pixels with flux above the 3.5σ detection limit. Saturated and extended sources were rejected from further consideration. We calibrated the coordinate system against the 2MASS point-source catalog (Skrutskie et al. 2006) for J and K_s bands separately, with typical fitting residuals of 0.″11. Duplicate sources from adjacent fields were removed. We cross-correlated the sources from the J-band catalog with the K_s-band catalog, requiring a separation of $<2''$ to be a match. Sources that are only detected in one band, either J or K_s, were rejected. The final near-infrared catalog contains 1571 objects.

The fluxes for these sources were extracted using a fixed 6 pixel radius aperture for all fields. To correct for the variable seeing, we derived an aperture correction factor for each image and applied it to the fluxes. Based on the 2MASS point-source catalog, we derived the absolute zero point for each individual field. For 19 fields, no 2MASS sources were covered; for these fields a zero point is derived based on the average of zero points in other fields at similar airmass. The completeness limit of the observations was found to be 20.6 ± 0.30 in the J band and 17.8 ± 0.30 in the K_s band; see Figure 2.

2.3. Cross-correlation of Optical and NIR Catalogs

The sources from the i'-band catalog were cross-correlated by coordinates with the sources from the JK_s catalog, requiring a separation of $<2''$ to be a match. The resulting final catalog of sources with detections in all three bands (hereafter "iJK_s catalog") contains 504 sources.

The spatial distribution of these 504 sources is shown in Figure 3 in comparison with the visual extinction map given by the COMPLETE project.[9] As seen in the figure, we have chosen the pointings of our observations to cover the high

[7] IRAF is distributed by the National Optical Astronomy Observatory, which is operated by the Association of Universities for Research in Astronomy, Inc., under cooperative agreement with the National Science Foundation.

[8] http://subarutelescope.org/Observing/Instruments/MOIRCS/imag_information.html

[9] http://www.cfa.harvard.edu/COMPLETE

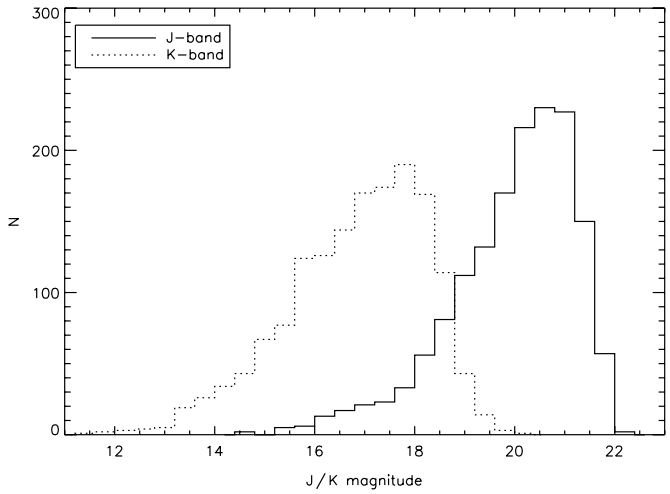

Figure 2. J-band and K_s-band histogram of the objects in our photometric catalog with J- and K_s-band data. The peaks at 20.6 and 17.8 mag indicate the completeness limit of the survey in J and K_s bands, respectively.

extinction contours of the L1688 core; however, parts of the region surveyed by Suprime-Cam were not covered in MOIRCS.

The majority of the iJK_s catalog objects are located outside the region with the highest A_V, at a typical A_V range of 5–15. At higher A_V, toward the center of ρ Oph, the lack of sources corresponds to a lack of i'-band detections due to the high A_V. At lower A_V, many objects are saturated in JK_s. As shown in Figure 3, the majority of the BD candidates are found in several distinct clumps at regions with low to moderate cloud extinction, $A_V = 5$–15, within the region covered by both the Suprime-Cam and MOIRCS imaging. Three of these regions are selected for multi-object follow-up spectroscopy (see Section 4), which showed that this apparent clustering is dominated by background objects. Thus, the distribution of the combined iJK_s catalog sources traces substructure in the extinction, and not in the distribution of young stellar objects (YSOs).

We convert the dynamic range and completeness limit of the i'-band and J-band surveys separately to mass sensitivity limits, by comparing with model evolutionary tracks DUSTY00 (Allard et al. 2001) and COND03 (Baraffe et al. 2003), described further in Section 3.1 and Figures 4 and 5.

The majority of i'-band magnitudes are between 18 and 25.5 mag, with the completeness limit at 24.15 mag. ρ Oph has significant and strongly variable extinction, with a typical minimum A_V of 5 mag, ranging up to 15–30 mag near the center of the cluster, and upward of 30 mag in the very center of the cluster (Ridge et al. 2006). For an A_V of 5, corresponding to $A_i = 3.45$ (Mathis 1990), the i'-band range of 18–25.5 mag corresponds to masses ranging between 0.002 and 0.068 $M_\odot$, with the completeness limit in the i' band corresponding to a mass ranging between 0.004 and 0.005 $M_\odot$ based on the 1 Myr COND03 and DUSTY00 models. At a moderate $A_V = 15$, the i'-band survey range corresponds to masses from 0.047 to more than 0.1 $M_\odot$ (outside model range), with the completeness limit corresponding to a mass sensitivity limit of 0.09–0.1 $M_\odot$.

The J-band survey was sensitive to magnitudes between 15 and 21.3, with a completeness limit of 20.6 mag. For $A_V = 5$ ($A_J = 3$; Mathis 1990), the 15–21.3 mag range corresponds to masses in the range of 0.001–0.034 $M_\odot$, with the completeness limit corresponds to masses of ~0.001–0.003 $M_\odot$. For an A_V of 15, the survey range corresponds to masses of 0.005–0.1 $M_\odot$, with the completeness limit corresponding to masses of 0.006–0.007 $M_\odot$.

In summary, the sensitivity of the i'-band and J-band surveys was such that they were complete down to below the substellar regime, for low to moderate A_V, while sensitivity in the upper mass range was different between the i' and J bands, due to the J band saturating at lower masses. However, particularly at large A_V, the survey was still not deep enough in the i' band to probe down into the substellar regime, and below.

2.4. Cross-correlation of Optical and 2MASS NIR Catalogs

To increase the dynamic range of the survey in the near-infrared, we retrieved additional JK_s photometry from the 2MASS point-source catalog (Skrutskie et al. 2006). We selected 2MASS sources located within the spatial coverage of our i'-band survey. The objects were further required not to be extended with the semimajor axis $>10''$, nor fall within the elliptical profile of such an extended source (xflag = 0), and not to be associated with known solar system objects (a-flag = 0) and detection quality flags in J and K_s bands of "A." The resulting 2MASS catalog was cross-correlated by coordinates with the i'-band catalog sources. We require a separation of $<2''$ to be a match. The final i' + 2MASS J-, and K_s-band catalog contains 264 sources. The majority of these sources were saturated in the MOIRCS data, as illustrated in Figure 4.

2.5. Spitzer Photometry

We retrieved the *Spitzer* IRAC and MIPS photometry of ρ Oph from the Legacy Program data archive available at the *Spitzer* Science Center, using the "High reliability catalog" (HREL) created by the "Cores to Disks" (*c2d*) Legacy team, made available at the SSC Web site.[10] The photometry from this catalog is used in Section 3.2 to search for candidate substellar objects with disks.

The *Spitzer* catalog was cross-correlated with the MOIRCS J+K_s-band catalog as well as the 2MASS catalog (see selection in Section 2.4). Here we require a separation of $<5''$ for a match, and the final catalog is restricted to the spatial area of the Suprime-Cam i'-band coverage ($246.415 \leqslant$ R.A. $\leqslant 247.085$, $-24.77 \leqslant$ decl. $\leqslant -24.275$). The resulting catalog contains 952 matches between MOIRCS and *Spitzer* and 1166 matches between *Spitzer* and 2MASS.

3. SELECTION OF CANDIDATE LOW-MASS SOURCES IN ρ Oph

3.1. iJK_s Candidate Selection

We initially selected low mass and BD candidates based solely on the (i', i'–J) color–magnitude diagram (CMD). Figure 4 shows the CMD constructed from the Suprime-Cam i'-band catalog and both the MOIRCS and the 2MASS J-, + K_s-band catalog. For comparison, the DUSTY00 (Allard et al. 2001) and COND03 (Baraffe et al. 2003) atmosphere model evolutionary tracks for an age of 1 Myr are overplotted, adjusted to the distance of ρ Oph of 125 pc. We converted the Cousins I band to the Sloan i' band using the transformation given by Jordi et al. (2006). The BD candidate selection cutoff in (i'–J) is shown in Figure 4 and was determined as a linear approximation of the 1 Myr COND03 track. Any object redder than this line is considered a candidate. This selection gives us 309 BD candidates based on our iJK_s catalog and an additional

[10] http://data.spitzer.caltech.edu/popular/c2d/20071101_enhanced_v1/oph/catalogs/

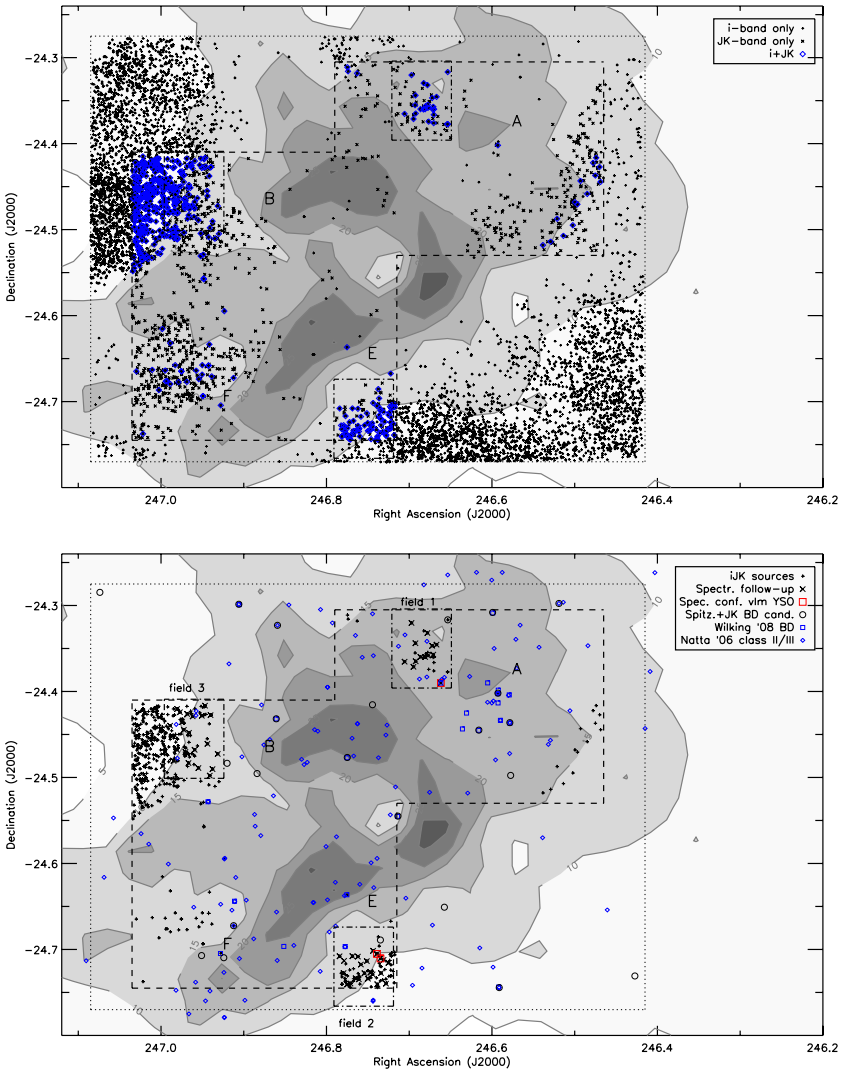

Figure 3. Spatial distribution of sources in ρ Oph. Contours are A_V = 5, 10, 15, 20, 25, 30, as derived from 2MASS by the COMPLETE project. Dotted line: *i*-band imaging coverage; dashed line: *J*- and K_s-band imaging coverage; dash-dotted line: MOIRCS spectroscopy fields. The locations of ρ Oph subclusters, as defined by the peaks of the DCO^+ dense cores from Loren et al. (1990), are indicated with letters. Top panel: *i* band indicated with "+," *J* and K_s bands indicated with "×," and iJK_s catalog sources indicated with diamonds. Bottom panel: iJK_s catalog sources indicated with "+," iJK_s catalog selected BD candidates with follow-up MOIRCS spectroscopy indicated with "×" (Section 4), and low-mass YSOs spectroscopically confirmed in this paper (Section 4.2) indicated with red large squares. Candidate BDs selected from JK_s + *Spitzer* photometry indicated with circles. Previously known BDs from Wilking et al. (2008) and class II/III sources from Natta et al. (2006) are indicated with small blue squares and diamonds, respectively.

(A color version of this figure is available in the online journal.)

228 sources based on the Suprime-Cam i'-band + 2MASS JK_s catalog. We obtained follow-up spectroscopy for a selection of the iJK_s catalog based BD candidates, as presented in Section 4.

The intrinsic J–K_s color of late-type objects is mostly independent of spectral type and luminosity and can be used to estimate the extinction for suspected cluster members. We adopt here an intrinsic color of J–K_s = 1.0 mag, which is consistent, within ±0.2 mag, with the empirical values for main-sequence dwarfs and giants with spectral type M (Bessell & Brett 1988), with the predictions from the evolutionary tracks COND03 (for 0.003–0.1 $M_\odot$), BCAH98 (for 0.03–0.5 $M_\odot$), and DUSTY00 (for 0.006–0.1 $M_\odot$), and with the colors of BDs in the 3 Myr old σ Ori star-forming region down to 0.013 $M_\odot$ (Caballero et al. 2007). For young objects with masses below the deuterium-burning limit, there are indications that the J–K_s color increases to 1.5 (Lodieu et al. 2006; Caballero et al. 2007); similarly, the presence of a circumstellar disk can increase the J–K_s color.

To estimate the extinction, we use the reddening law from Mathis (1990) with R_V = 4. Figure 5 shows the (J, J–K_s) CMD for the sample of 309+228 i'-band + MOIRCS and 2MASS catalog derived BD candidates. The reddening path is indicated by solid and dashed lines, and the intrinsic color indicated by a vertical dotted line. The 1 Myr COND03 evolutionary track is used for the mass estimate based on the dereddened *J*-band magnitude. We obtain visual extinctions of A_V = 3–16 for the MOIRCS sources and A_V = 2–34 for the 2MASS sources.

The main errors in the extinction estimates are the uncertainties in the estimate of the intrinsic colors (accurate to within 0.2 mag in J–K_s) and the possible excess emission due to disks and accretion (<1 mag in J–K_s; see Meyer et al. 1997), particularly for the sample selected based on *Spitzer* MIR excess in Section 3.2. Wilking et al. (2008) list 316 L1688 association members known in 2008 January, out of which 152 show infrared excess indicative of the presence of a disk (indicated with "B2ex," "B4ex," and "Mex" in their Table 1). This illustrates

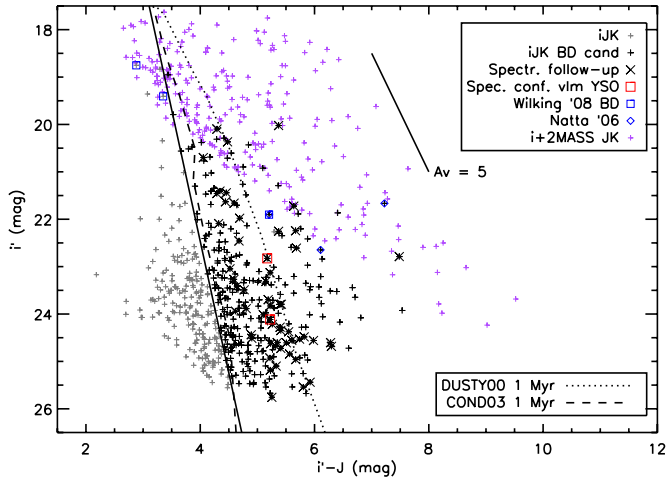

Figure 4. CMD in (i', i'–J). Sources from the Suprime-Cam and MOIRCS iJK_s catalog are indicated with light "+" symbols, while BD candidates based on iJK_s are indicated with dark "+" symbols. Sources from the Suprime-Cam and 2MASS catalogs are indicated with purple "+" symbols. Spectroscopy follow-up targets are indicated with "×," two confirmed very low mass YSOs with large red squares. Previously known BDs from Wilking et al. (2008) are indicated with small blue squares, class II/III sources from Natta et al. (2006) are indicated with small blue diamonds. Atmosphere model isochrones for age 1 Myr are overplotted for DUSTY00 (Allard et al. 2001) and COND03 (Baraffe et al. 2003). The solid line denotes the BD candidate selection cutoff.

(A color version of this figure is available in the online journal.)

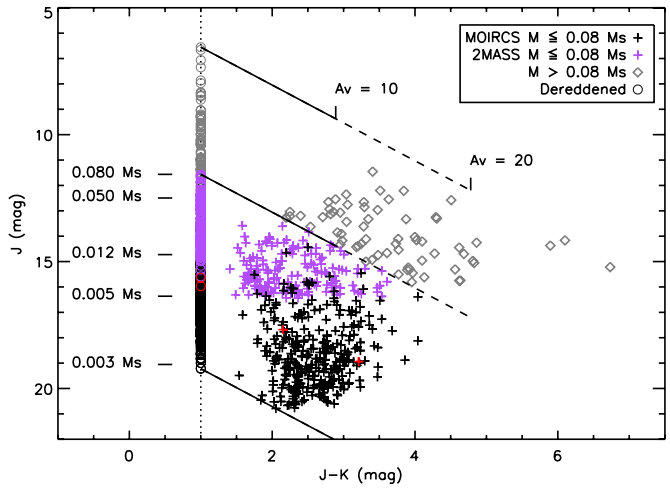

Figure 5. CMD in (J, J–K_s), constructed from the MOIRCS and 2MASS photometry, for the BD candidates selected from the iJK_s catalog and the i-band + 2MASS catalog. Solid and dashed lines indicate visual extinction of 10 and 20 mag from the assumed intrinsic J–K_s of 1 (vertical dotted line). "+" and diamond symbols indicate the MOIRCS and 2MASS photometric points, circles are dereddened in J. The two very low mass candidates confirmed by MOIRCS spectroscopy are included with red symbols.

(A color version of this figure is available in the online journal.)

that a substantial fraction of the L1688 members may show enhanced K_s-band flux due to excess emission from the dust in the disk. We conservatively estimate that our typical uncertainty in A_V is in the range of ± 1 mag for most sources, but may be up to 5 mag if disk excess is present. We note that BDs with disks typically have only little color excess in the near-infrared.

The estimated range of visual extinction is in good agreement with the ρ Oph extinction map as derived from 2MASS imaging observations by the COMPLETE team.

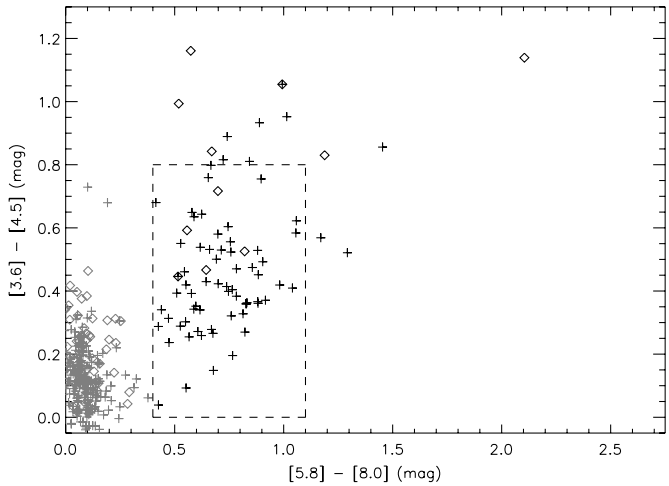

Figure 6. Color–color diagram in (3.6–4.5, 5.8–8.0), constructed from *Spitzer* IRAC photometry, for 2MASS (crosses) and MOIRCS (diamonds) sources with a *Spitzer* match. The dashed line denotes the area where class II objects are located, based on Allen et al. (2004). All sources selected as having significant NIR excess are indicated in black.

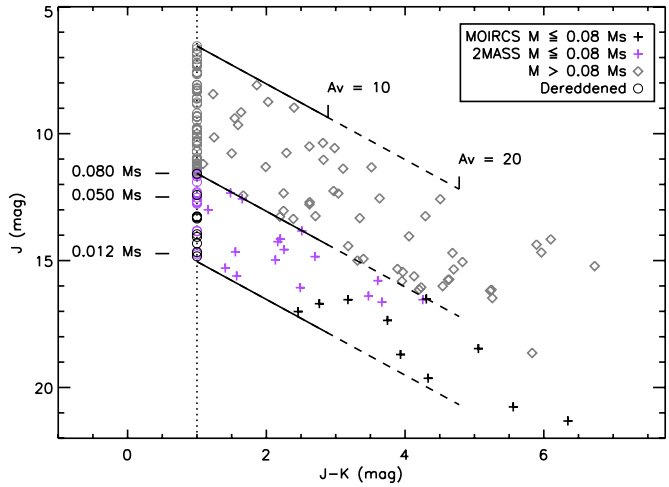

Figure 7. CMD in (J, J–K_s), constructed from the MOIRCS and 2MASS photometry, for the sources with *Spitzer* NIR excess. Solid and dashed lines indicate visual extinction of 10 and 20 mag from the assumed intrinsic J–K_s of 1. "+" and diamond symbols indicate the MOIRCS and 2MASS photometric points, circles are dereddened in J.

(A color version of this figure is available in the online journal.)

3.2. JK_s + *Spitzer* Candidate Selection

As the i'-band observations were not complete in the central parts of L1688 with high A_V, we selected a second sample of candidate substellar mass objects with disks based on the mid-infrared photometry from the *Spitzer Telescope*, restricted to the spatial area of the i'-band coverage (see Section 2.5). Figure 6 shows a color–color diagram of the four IRAC bands for the MOIRCS and 2MASS sources. For 11 MOIRCS sources and 72 2MASS sources, the IRAC colors are consistent with or redder than sources with a circumstellar disk. The presence of a circumstellar disk is taken as a confirmation of youth and membership in the ρ Oph cluster.

Figure 7 shows the (J, J–K_s) CMD for the sample of 11 MOIRCS and 72 2MASS sources with excesses in the *Spitzer* data. Based on the CMD and the DUSTY00 atmospheric model, we find 10 MOIRCS BD candidates and 17 2MASS

BD candidates with $M < 0.08\,M_{\odot}$, assuming an intrinsic BD photosphere J–K_s color of 1 mag. These 10 + 17 candidates are listed in Table 1. Among this selection of 27 BD candidates, 16 are new, while 11 are previously spectroscopically confirmed BDs. If we assume an additional 1 mag J–K_s excess due to the presence of a circumstellar disk (intrinsic J–$K_s = 2$), then the number of candidates increases to 11 MOIRCS and 39 2MASS sources.

For this sample of JK_s + *Spitzer* excess sources, estimates of the extinction are derived as described in Section 3.1. The visual extinction obtained for this sample is $A_V = 0$–30 and is given in Table 1.

4. MULTI-OBJECT SPECTROSCOPIC FOLLOW-UP OF CANDIDATES

4.1. Observations and Data Reduction

We used MOIRCS to carry out multi-object spectroscopy for 59 BD candidates selected from the i', J, K_s photometry (see Section 3), composed of 58 new candidates and 1 previously known BD candidate, GY 84. The targets were covered in three fields, centered on the areas with highest density of candidates, indicated in Figure 3. The three fields are numbered by increasing R.A. as fields 1, 2, and 3. Two of these candidates are located only 1.″5 apart from each other in α, so that they can be covered in one slit. In addition, we observed one confirmed young M dwarf, GY 84, published by Natta et al. (2006), which falls into one of our fields.

Pre-imaging for the MOS masks in the K_s band was obtained in 2009 April. We used slits which are 0.″9 wide and 9″–12″ long. The spectroscopy run was carried out in two nights on 2009 May 30 and 31, using the grisms HK500, which covers the H and K_s bands. The second half of the first night was lost due to technical problems; as a result the exposure time for field 1 is lower than intended. The total on-source time was 30, 140, and 150 minutes for fields 1–3, split in shorter exposures of 5 or 10 minutes. The typical seeing during these nights was 0.″5, as determined in the focusing procedure. The average airmass for the three fields is 1.8, 1.5, and 1.5.

Before and after the ρ Oph masks, we observed A0 stars through one of the science masks for flux calibration and extinction correction; these exposures required de-focusing to prevent saturation. In total two A0 stars were observed in night 1 and seven in night 2, at various airmasses. For each mask, we obtained series of domeflats with lamp on and off for calibration purposes. Between the single exposures, the telescope was moved so that the targets shifted by 2.″5 along the slit (nodding) to facilitate sky subtraction.

The MOS data were reduced following mostly the recipes outlined in Scholz et al. (2009). After subtracting the nodded exposures to remove the background, the images were divided by a normalized flat-field. Frames from the same nodding position were co-added using the median and a sigclip routine to remove cosmic ray events. This gives us two final frames for each chip and mask, from which the spectra were extracted using *apall* in IRAF. All candidates are well detected. The wavelength solution was derived from the OH lines in the unreduced frames, for each object separately. The typical rms of the fit was 2–3 Å, well below the resolution. All spectra were binned to 40 Å pixel^{-1}, corresponding to a resolution of 500 at 2.0 μm. The two nodded spectra for the same object were co-added. The standard star spectra were treated in exactly the same way as the science frames.

After background subtraction, the science frames still show 5%–10% residuals from the OH lines. The reason is that ρ Oph was observed at relatively high airmasses, so that consecutive exposures differ in airmass by as much as 0.1. However, the extraction with *apall* includes a background fit perpendicular to the dispersion direction which reliably removes the residuals. We made sure that the final science spectra are not significantly affected by OH lines.

The corrections for the broad telluric absorption features between the near-infrared bands and for the instrument response were done in one step, using the A0 standard stars. The A0 standard star spectra were divided by a library spectrum of an A0 star (Pickles 1998), obtained from the ESO Web site.[11] The resulting calibration spectra show the combined effects of telluric absorption and response. Two out of the nine spectra differ significantly from the average; in one case, probably due to effects of saturation, the other one has a usually large J–K_s color of 0.2 (obtained from 2MASS) which might indicate the presence of a dust shell. Both were not considered for the calibration.

Most of the differences in the remaining seven A0 spectra are caused by the variable airmass. For each wavelength bin, we fit the fluxes linearly as a function of airmass and extrapolated to airmass of 1.0. While the extinction coefficients are consistent with the standard extinction law in the wavelength domain 1.45–1.8 μm and 2.05–2.3 μm, they vary strongly and irregularly in the water absorption features outside these bands, which cannot be reliably calibrated. The spectrum for airmass 1.0 was smoothed and fit with a second-order polynomial over the H and K_s bands. The result is our final calibration spectrum. All science spectra were extinction corrected using the coefficients derived from the standard spectra and the average airmass and then divided by the calibration spectrum.

4.2. Spectral Analysis

Our goal is to identify young sources with spectral types later than M5. As outlined in detail in Scholz et al. (2009), these objects show a characteristic spectral shape in the near-infrared. In particular, their spectra have a clear peak in the H band (Cushing et al. 2005). This feature is caused by water absorption on both sides of the H band. The depth of these features depends strongly on effective temperature. While the H-band peak appears round in old field dwarfs, it is unambiguous triangular in young, low-gravity sources, likely due to the effects of Collisional Induced Absorption (Kirkpatrick et al. 2006; Witte et al. 2009). In addition, young BDs are expected to have flat or increasing K_s-band spectra with CO absorption bands at $\lambda > 2.3\,\mu$m.

In a first step, we visually inspect our spectra to search for the characteristic signature of young BDs. Three objects exhibit the features described above, including the object GY 84 from Natta et al. (2006); these objects are listed in Table 2 and their spectra are shown in Figure 8. For six objects, the signal-to-noise ratio is too low to conclusively determine their nature. The remaining 50 objects have smooth spectra with mostly decreasing K_s-band slope.

In a second step, we estimate the effective temperatures of the BD candidates by fitting model spectra from the DUSTY series (Allard et al. 2001), following the procedure outlined in Scholz et al. (2009). We used the extinction as determined from the

[11] http://www.eso.org/sci/facilities/paranal/instruments/isaac/tools/~lib/index.html

Table 1
Likely Substellar Members with Disks in ρ Oph from *Spitzer* + JK_s Photometry

No.	R.A. (J2000)	Decl. (J2000)	J (mag)	K_s (mag)	IRAC1 (mJy)	IRAC2 (mJy)	IRAC3 (mJy)	IRAC4 (mJy)	A_V (mag)	JK_s Phot.	Identifiers	References BD Candidacy
1	16 26 18.58	−24 29 51.4	17.36	13.61	3.93	4.08	4.58	5.44	14.5	MOIRCS	BKLT J162618-242951	···
2	16 26 22.28	−24 24 07.1	16.70	13.94	3.10	4.26	5.53	9.21	9.3	MOIRCS	GY 11	WGM99,CTK00,N02
3	16 26 36.84	−24 19 00.1	17.01	14.55	1.10	2.05	3.70	3.50	7.7	MOIRCS	BKLT J162636-241902	···
4	16 26 56.37	−24 41 20.5	18.70	14.77	1.01	0.99	1.06	1.07	15.5	MOIRCS	···	···
5	16 26 58.66	−24 24 55.6	19.64	15.30	3.72	5.17	5.65	5.84	17.6	MOIRCS	AOC J162658.65-242455.5	···
6	16 26 59.04	−24 35 56.9	16.51	12.21	14.20	13.70	11.60	10.40	17.5	MOIRCS	GY 172	···
7	16 27 32.15	−24 29 43.6	18.47	13.41	8.28	9.14	9.16	8.53	21.6	MOIRCS	GY 287	···
8	16 27 38.95	−24 40 20.7	16.54	13.36	15.80	26.70	38.20	53.20	11.5	MOIRCS	GY 312	···
9	16 27 41.80	−24 42 34.7	21.32	14.97	1.64	2.03	2.29	2.43	28.3	MOIRCS	···	···
10	16 27 48.24	−24 42 25.8	20.76	15.21	1.21	2.21	3.64	14.10	24.1	MOIRCS	AOC J162748.24-244225.6	···
11	16 25 42.54	−24 43 51.1	15.61	14.03	0.99	0.66	0.47	0.39	3.0	2MASS	BKLT J162542-244350	···
12	16 26 04.58	−24 17 51.5	15.79	12.19	10.20	9.89	8.98	11.30	13.8	2MASS	BKLT J162604-241753	···
13	16 26 18.82	−24 26 10.5	14.84	12.14	10.50	11.50	13.90	20.50	9.0	2MASS	CRBR 2317.3-1925	WGM99
14	16 26 21.53	−24 26 01.0	12.57	10.92	25.00	20.30	19.30	19.10	3.4	2MASS	GY 5	WGM99,N02
15	16 26 21.90	−24 44 39.8	12.34	10.86	28.80	26.60	23.80	26.40	2.6	2MASS	GY 3	N02,W05
16	16 26 23.81	−24 18 29.0	16.07	13.58	2.72	2.27	1.79	1.62	7.9	2MASS	CRBR 2322.3-1143	CTK00
17	16 26 27.81	−24 26 41.8	14.26	12.09	9.52	8.74	7.78	7.38	6.2	2MASS	GY 37	WGM99,W05
18	16 26 37.81	−24 39 03.2	14.98	12.85	4.47	3.92	3.35	3.21	6.0	2MASS	GY 80	···
19	16 26 51.28	−24 32 42.0	15.30	13.89	1.55	1.31	1.34	1.24	2.2	2MASS	GY 141	LLR97,CTK00
20	16 27 05.98	−24 28 36.3	16.64	12.97	5.43	5.16	5.32	5.37	14.1	2MASS	GY 202	WGM99,LR99,CTK00
21	16 27 26.22	−24 19 23.0	16.40	12.93	6.20	6.29	6.48	6.83	13.1	2MASS	BKLT J162726-241925	···
22	16 27 26.58	−24 25 54.4	13.00	11.84	10.30	10.20	9.78	12.00	0.9	2MASS	GY 264	W05
23	16 27 37.42	−24 17 54.9	14.15	11.95	11.20	10.20	10.20	11.70	6.4	2MASS	ISO-Oph 160	N02
24	16 27 38.95	−24 40 20.7	16.54	12.29	15.80	26.70	38.20	53.20	17.2	2MASS	ISO-Oph 165	···
25	16 27 40.84	−24 29 00.7	14.66	13.10	2.78	2.28	2.22	2.64	2.9	2MASS	GY 320	···
26	16 27 46.29	−24 31 41.2	13.83	11.32	17.60	15.70	14.80	18.60	8.0	2MASS	GY 350	N02
27	16 28 17.74	−24 17 05.0	14.57	12.31	7.40	6.17	5.20	4.29	6.6	2MASS	BKLT J162817-241706	···

References. For papers spectroscopically confirming BD candidacy: WGM99: Wilking et al. 1999; CTK00: Cushing et al. 2000; N02: Natta et al. 2002; W05: Wilking et al. 2005. References for identifiers: GY: Greene & Young 1992; CRBR: Comeron et al. 1993; BKLT: Barsony et al. 1997; ISO-Oph: Bontemps et al. 2001; AOC: Alves de Oliveira & Casali 2008.

Table 2
Probable Low Mass and Substellar Mass Members of ρ Oph, with MOIRCS Spectroscopy Follow-up

No.	R.A. (J2000)	Decl. (J2000)	i' (mag)	J (mag)	K_s (mag)	$T_{\rm eff}$ (K)	A_V	Notes
1	16 26 56.33	−24 42 37.8	21.24	17.68	15.53	2500	5	SONYC-RhoOph-1
2	16 26 57.36	−24 42 18.8	22.53	18.94	15.73	3100	10	SONYC-RhoOph-2
3	16 26 38.82	−24 23 24.7	21.10	15.10	sat	3400	14	GY 84

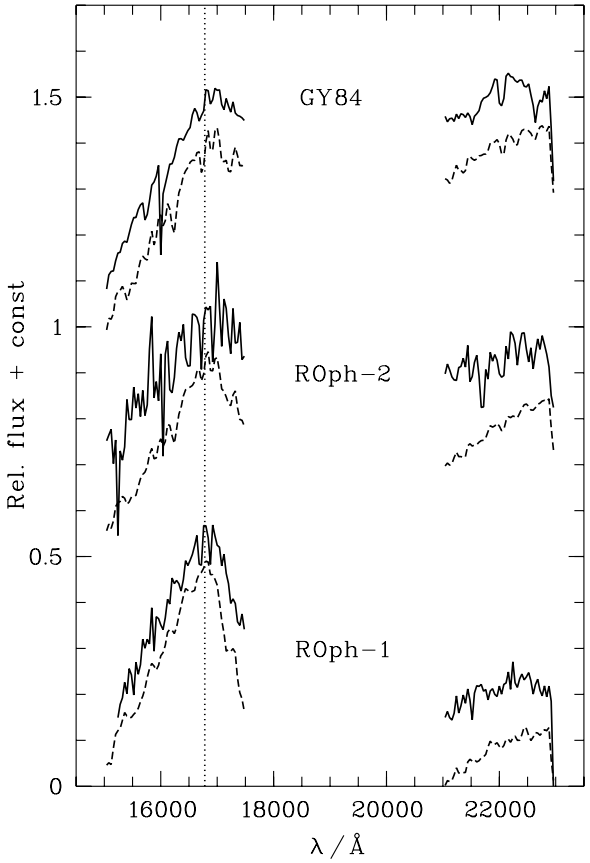

Figure 8. MOIRCS spectra (solid) of candidate substellar objects in ρ Oph, with best-fit reddened model (dashed) with a $T_{\rm eff}$ of 2500 K, 3100 K, and 3400 K; offsets were applied for clarity.

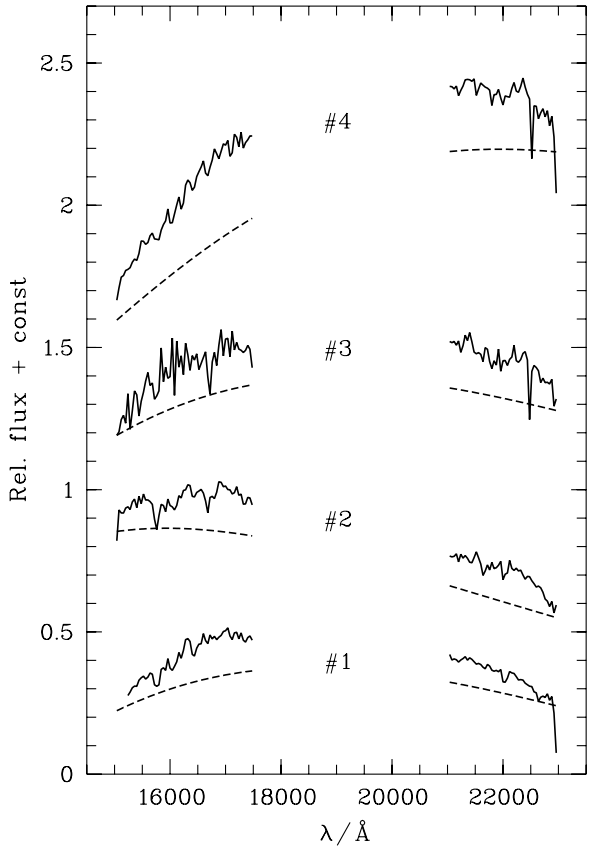

Figure 9. Example MOIRCS spectra (solid) of sources in ρ Oph which are not substellar candidates, with overplotted reddened blackbodies (dashed) with $T_{\rm eff}$ ranging from 3000 to 4000 K; offsets were applied for clarity. Objects 1 and 4 in this plot are known in the literature as BKLT J162759-242912 and BKLT J162708-244227 (Barsony et al. 1997).

J–K_s color (see Section 3.2). For GY 84 the value of $A_V = 14$ published by Natta et al. (2006) is used. The results are listed in Table 2. We find best-fitting effective temperatures of 2500 and 3100 K for our two candidates, here named SONYC-RhoOph-1 and SONYC-RhoOph-2, and a $T_{\rm eff} = 3400$ K for GY 84, corresponding to spectral types M9, M5, and M3, respectively. SONYC-RhoOph-1 is confirmed as a newly found BD. Based on the COND03 and DUSTY00 evolutionary tracks for 1Myr, it has a mass estimate of 0.015–0.02 $M_\odot$, marking it as one of the lowest mass objects in ρ Oph. The temperatures we derive for GY 84 and SONYC-RhoOph-2 are too high to classify them as BDs. For comparison, Natta et al. (2006) list $T_{\rm eff} = 2900$ for GY 84, derived by converting the J-band magnitude to luminosity and comparing with theoretical evolutionary tracks. The model spectrum with 2900 K however clearly does not match the observed spectrum.

The remaining sources, which are not BDs and have sufficient signal-to-noise ratio, exhibit smooth, featureless spectra, which make it difficult to constrain their nature. The overwhelming majority of these objects are expected to be background late-type objects giant or dwarf stars. Some of them could be embedded YSOs with spectral types earlier than M, although we do not have any evidence for youth. We note that this sample contains 14 objects[12] from the BKLT catalog, a near-infrared survey by Barsony et al. (1997) without spectroscopic follow-up. Four examples of these featureless spectra are shown in Figure 9.

4.3. Comparison with Other Studies

The iJK_s-selected catalog of candidate BDs is compared with the list of 24 candidate BDs published in Wilking et al. (2008, hereafter W08). Twenty-one objects fall within the spatial coverage of both the i'-band and the J+K_s-band imaging; three objects are not covered in i' and/or J band (GY 141, Oph-160, and Oph-193). Of the 21 covered, 12 are saturated (CRBR14, CRBR31, GY 3, GY 5, GY 10, GY 37, GY 64, GY 84, GY 204,

[12] BKLT J162640-242046, J162646-242155, J162654-244254, J162655-244242, J162656-244338, J162658-244342, J162703-244400, J162704-244422, J162708-244227, J162743-242822, J162745-242952, J162748-242542, J162750-242544, and J162759-242912.

GY 264, GY 310, GY 350, and GY 202), 3 are undetected in the i' band (CRBR15, CRBR23, and GY 258), 1 is undetected in both i' and J bands (GY 31), and 1 is not properly detected in the J band due to strong distortion from a nearby bright source (see Section 2.2). Three of the 21 are recovered in the iJK_s catalog, GY 11, GY 201, and GY 325, indicated in Figure 4. Of these 3, only 1 is recovered as a BD candidate (GY 11) in the (i', i'–J) CMD selection (Section 3.1), while the other 2 (GY 201, GY 325) are blueward of the selection cutoff.

We also compare our candidate BDs to the Natta et al. (2006) sample of objects with evidence of a circumstellar disk and measurements of accretion. Three sources are covered in the iJK_s catalog, ISO033 (=GY11 in W08), ISO165, and ISO169b, all three are recovered as BD candidates.

We compare our study with the recent paper by Alves de Oliveira et al. (2010), hereafter referred to as A10. Both studies use JHK_s near-infrared photometry; in this paper, i-band photometry is added for the entire survey area, while A10 added archive i-band and z-band photometry for a subset of their JHK_s sources. Both studies select candidate BDs from color–magnitude and color–color diagrams based on predictions by evolutionary models. Two of the six new BDs found by A10 are covered in our iJK_s survey area, but were not recovered in our iJK_s catalog, due to saturation in the J band in one case and extended emission interference in the i' band in the other case. Our one new spectroscopically confirmed BD (R.A. 246.734, decl. −24.711) appears to have been covered by A10 (based on their Figure 4), but is not reported as a candidate Rho Oph member (A10, Table 4).

5. DISCUSSION: BROWN DWARF POPULATION IN ρ Oph

In the following section, we use our survey results in combination with literature data to put limits on the total number of substellar objects in the ρ Oph star-forming region. We would like to preface this analysis with a cautionary note: ρ Oph with its high and strongly varying extinction is a difficult field to search for BDs. All existing surveys have to be considered incomplete. The three key requirements to achieve a full census of BDs in this area are (1) observations in multiple bands, (2) combination of different survey strategies (e.g., broadband versus narrowband surveys), and (3) comprehensive spectroscopic follow-up.

Our SONYC survey provides new constraints on the substellar population in ρ Oph. We have used two different strategies. In a first step, we identify objects with iJK_s photometry. As it turns out, this selection is heavily affected by background contamination and is not effective in the high extinction areas. It mostly covers the edges of the dense cloud core. In a second step, we look for *Spitzer*/IRAC color excess due to a disk in objects from our JK_s database. This sample should be dominated by young objects in ρ Oph, but it is not clear what fraction is substellar. Since we do not require an optical counterpart, this selection also traces the dense cloud areas. Thus we provide two complementary approaches to identify BDs.

Our iJK_s survey is certainly not complete for substellar objects. In the high extinction areas, the i'-band data are not deep enough (although deeper than all other previously published optical surveys in this region). In the low extinction areas, more massive BDs can be saturated in the J and K_s bands, as evidenced by the significant number of literature BDs missing in our catalog (Section 4.3). Our sample identified from *Spitzer* color excess is missing objects without disks.

The previous surveys in the literature are subject to various biases as well. For example, the 20 objects observed by Wilking et al. (1999) have been selected from various near-infrared surveys which yield a much larger initial sample. Their color criterion favors objects "near the surface of the cloud" (Wilking et al. 1999) and will not find deeply embedded sources. The objects confirmed by Natta et al. (2002) as BDs in ρ Oph have been selected from the ISOCAM survey by Bontemps et al. (2001) using a combined extinction (i.e., color) and luminosity criterion. This approach will by definition not be able to find the objects without disks nor the ones with high extinctions. A similar argument can be made for the objects confirmed by Jayawardhana & Ivanov (2006) and Allers et al. (2007), which were selected from *Spitzer* data. This simply illustrates that only the combination of multiple survey strategies can provide a more complete census.

One of the key features of our survey is extensive follow-up spectroscopy for our primary candidates from the iJK_s database. Out of 504 objects, 309 were selected with colors consistent with substellar or planetary masses; for 58 of these candidates, and 1 known YSO, we obtained spectra. Only three of these turn out to be bona fide YSOs; one is a newly discovered young BD. Assuming that we selected the spectroscopy candidates in an unbiased way, we expect that the total catalog contains not more than a handful (∼5) of new substellar objects.

The latter estimate is only a lower limit for the actual number of new BDs in our catalog. The spectroscopy fields were deliberately placed in regions with strong clustering. As the spectroscopy shows, most of the objects in these regions are background stars, i.e., the clustering reflects substructure in the extinction of the cloud. In areas with higher or lower extinction, we expect to have less contamination by background objects because they are either not visible or do not pass our color criterion. Taking this into account, we make a second estimate of the total number of BDs in the iJK_s catalog based on the success rate and spatial coverage of the follow-up spectroscopy while we assume a spatially homogeneous population of BDs. Our three MOS fields cover 72 arcmin^2 out of ∼616 arcmin^2 (0.171 deg^2) in the total i+JK_s survey (∼12%). We obtained spectra for 59 out of the 159 iJK_s candidates (∼37%) located within the area of the MOS fields and find one bona fide BD. Scaling to the total area of our survey yields an estimate of 24 BDs. We note that this estimate is taken as an order of magnitude estimate, since it has a large uncertainty (1σ confidence interval of 5–74, assuming binomial distribution), and moderate clustering in the YSO population (Bontemps et al. 2001) may further increase the estimate. We conclude that despite the low yield of our spectroscopy campaign our database might still contain a substantial number of new BDs. Spectroscopy covering the full field is required to clarify this.

We demonstrate that the available *Spitzer* data contain more objects than previously known that might be BDs in ρ Oph. By combining our deep JK_s data with the *Spitzer* C2D catalog, we select 10 candidates with mid-infrared color excess and near-infrared colors indicative for a substellar mass, of which 1 is a previously spectroscopically confirmed BD. In addition, 17 objects were found with 2MASS JK_s data in combination with *Spitzer* data, using the same approach, of which 10 objects were previously spectroscopically confirmed BDs. The 17 new candidates exhibit a wide range of visual extinctions from 0 to 20 mag. In particular, the high-extinction objects constitute a parameter regime not covered sufficiently in previous surveys.

Table 3
Spectroscopically Confirmed Brown Dwarfs Within i'-band Survey Area of ρ Oph

Name(s)	R.A. (J2000)	Decl. (J2000)	Indicator(s) of Youth	SpT	References
CRBR 2317.3-1925/CRBR 14/ISO-Oph-23	16 26 18.82	−24 26 10.5	CO bands+A_V, mid-IR excess	M7.5,M5.5,M7	WGM99,LR99,N02
GY 5	16 26 21.54	−24 26 01.0	CaH,TiO, CO bands+A_V, mid-IR exc.	M5.5,M7,M6	W05,WGM99,N02
GY 3	16 26 22.05	−24 44 37.5	CaH, TiO, mid-IR excess	M8,M7.5	W05,N02
GY 10	16 26 22.17	−24 23 54.4	CO bands+A_V	M8.5,M6.5	WGM99,LR99
GY 11	16 26 22.28	−24 24 09.3	H_2O abs., CO bands+A_V	M6.1,M6.5,M8.5	CTK00,WGM99,N02
CRBR 2322.3-1143/CRBR 31	16 26 23.78	−24 18 31.4	H_2O abs.	M6.7	CTK00
GY 37	16 26 27.83	−24 26 42.6	CaH, TiO	M5,M6	W05,WGM99
GY 59	16 26 31.37	−24 25 30.3	CO bands+A_V	M3.75,M6,M5	W05,WGM99,LR99
GY 64	16 26 32.56	−24 26 36.9	H_2O abs., CO bands+A_V	M7.0,M8	CTK00,WGM99
GY 84	16 26 38.80	−24 23 22.7	CO bands+A_V, H_2O abs.	M6,M3[a]	WGM99, This work
CFHTWIR-Oph 34	16 26 39.92	−24 22 33.6	H_2O absorption	M8.25	A10
GY 141	16 26 51.42	−24 32 42.7	H_α, H_2O abs.	M8.5,M8.0	LLR97,CTK00
SONYC-RhoOph-1	16 26 56.33	−24 42 37.8	H_2O absorption	M9[a]	this work
GY 202	16 27 06.00	−24 28 37.3	H_2O abs., CO bands+A_V	M5.7,M7,M6.5	CTK00,WGM99,LR99
GY 204	16 27 06.58	−24 41 47.9	CaH, TiO, mid-IR excess	M5.5,M6	W05,N02
MARSH10-4450[b]	16 27 25.35	−24 25 37.5	CH_4, H_2O absorption	Early T	M10
GY 264	16 27 26.58	−24 25 55.1	CaH, TiO	M8	W05
ISO-Oph 160	16 27 37.30	−24 17 56.4	Mid-IR excess	M6	N02
GY 310	16 27 38.67	−24 38 38.2	CO bands+A_V	M8.5,M7,M6	WGM99,LR99,N02
CFHTWIR-Oph 96	16 27 40.84	−24 29 00.8	H_2O absorption	M8.25	A10
GY 350	16 27 46.36	−24 31 41.6	Disk excess	M6	N02

Notes.
[a] Spectral type estimate based on $T_{\rm eff}$—SpT scale from Table 8 of Luhman et al. (2003).
[b] Provisional name chosen in this paper; no entry for this source exists in SIMBAD.
References. LLR97: Luhman et al. 1997; WGM99: Wilking et al. 1999; LR99: Luhman & Rieke 1999; CTK00: Cushing et al. 2000; N02: Natta et al. 2002; W05: Wilking et al. 2005; W08: Wilking et al. 2008; A10: Alves de Oliveira et al. 2010; M10: Marsh et al. 2010. References for identifiers: GY: Greene & Young 1992; CRBR: Comeron et al. 1993; ISO-Oph: Bontemps et al. 2001.

Again, this sample requires full spectroscopy follow-up for a more detailed characterization.

In Table 3, we provide a list of the spectroscopically confirmed BDs in the literature, including our new object, restricted to our i'-band survey area ($246.415 \leqslant$ R.A. $\leqslant 247.085$, $-24.77 \leqslant$ decl. $\leqslant -24.275$). The main criteria for an object to appear in this list are (1) spectral type later than M6 or alternatively effective temperature below 3000 K and (2) evidence for youth (e.g., disk excess, spectral features indicative of low gravity). We include sources with multiple spectroscopically determined spectral type estimates, if at least one is M6 or later. To date, 21 objects fulfill these criteria. As outlined above in detail, this number is almost certainly a lower limit to the full number of BDs in ρ Oph. The table should be seen as a starting point in establishing a more complete census. We did not include the three BDs from Allers et al. (2007) as those are located outside our survey area. We note the inclusion of the spectroscopically confirmed early T dwarf found by Marsh et al. (2010), for which evidence for youth is found in low-gravity features. This may be the lowest mass object identified in ρ Oph so far, although its cluster membership is still in question as Alves de Oliveira et al. (2010) note that they find a different K_s magnitude than Marsh et al. (2010), based on which the distance estimate would place the object at 137–217 pc, behind the ρ Oph cloud. Finally, we note that 16 of the 21 objects in Table 3 are in agreement with Alves de Oliveira et al. (2010, Table 7). We do not list five of their BDs outside our survey area: ISO-Oph 193, CFHTWIR-Oph 4, 47, 57, and 106. We do list five BD candidates that they do not: the newly found SONYC-RhoOph-1 and MARSH10-4450, as well as the three borderline cases GY 37, GY 59, and GY 84, that have multiple conflicting spectral type estimates in the literature.

Our sample of candidates identified from *Spitzer* excess allows us to estimate an upper limit for the number of missing BDs in ρ Oph. Our MOIRCS JK_s survey area covers 19 of the 21 spectroscopically confirmed BDs from Table 3. In the same area are additional 16 new BD candidates with disks (see Table 1). Assuming a disk fraction of ∼67% (Jayawardhana et al. 2003), the upper limit for BD candidates in this area is $\sim 16 \times 1.5 = 24$, and subsequently, an upper limit on total number of BDs would be 24 + 19 = 43, roughly twice the number already confirmed with spectroscopy within our JK_s survey area. In other words, the current census of confirmed BDs might still miss a few tens of substellar objects.

It is premature to derive the substellar IMF in ρ Oph. However, based on the currently available data we can estimate the number of low-mass stars ($0.1\,M_\odot < M < 1.0\,M_\odot$) in relation to the number of BDs ($M < 0.1\ M_\odot$), a ratio that has been derived for a number of star-forming regions (Andersen et al. 2008; Scholz et al. 2009).

Bontemps et al. (2001) provide constraints on the stellar mass function in this region, complete down to below $0.1\ M_\odot$. From their Figure 8, we infer a lower limit of ∼80 stars in the given mass range. Taking into account, an estimated binarity of ∼29% (Ratzka et al. 2005) would increase this number to about 103. Wilking et al. (2008) summarized a list of 316 L1688 association members with at least a K_s-band 2MASS detection, as well as one or more signs of association membership, and 169 out of 316 sources have an optical and/or IR spectral type estimate. Of these 169, 19 association members are BDs with one or more spectral type estimations of M6 or later, while 140 are low-mass stars with spectral type estimates between G2 and M6 ($0.1\ M_\odot < M < 1.0\ M_\odot$). Combining mid- and near-infrared as well as X-ray data, these are the most complete estimates for

the stellar population in ρ Oph to date. Making the reasonable assumption that the stellar sample is more complete than the brown dwarf sample, and adopting a range of 103–140 in the number of stellar sources, and 19 brown dwarfs, then an upper limit for the ratio low-mass stars to BDs is 5–7. Depending on how many BDs the current census is missing, this ratio might be as low as ∼3. As it stands now, the observed ratio is fully in line with the literature values for most other young clusters (3.3–8.5; Andersen et al. 2008), although significantly higher than the value we have obtained for NGC1333 (1.5; Scholz et al. 2009). Note that the values quoted by Andersen et al. (2008) should be treated as upper limits as well, since they are limited to BDs with $M > 0.03\ M_{\odot}$. Thus, there is no reason to believe that ρ Oph has a substellar IMF significantly different from other star-forming regions.

6. CONCLUSIONS

1. Large-scale, optical+near-infrared imaging surveys with Suprime-Cam and MOIRCS have been used to create a catalog of sources, reaching completeness limits of 24.2 in the i'-band, 20.6 in the J band, and 17.8 in the K_s band. The spatial coverage of our i'+JK_s survey is 0.171 deg^2 and covers the L1688 core in i', J, and K_s bands.
2. In terms of object masses for members of ρ Oph, the survey completeness limits correspond in the i' band to mass limits of 0.004–0.1 $M_{\odot}$and in the J band to mass limits of 0.001–0.007 $M_{\odot}$, for extinction ranges of A_V = 5–15, based on the COND03 and DUSTY00 evolutionary tracks.
3. From the optical + near-infrared photometry, 309 objects were selected as candidate substellar and planetary-mass cluster members. Fifty-eight of these objects, and one additional previously known BD candidate, were targeted for follow-up spectroscopy. Based on multi-object spectroscopy in H and K_s bands, using the water absorption features in the H band, 1 of the 58 new candidates was confirmed as a substellar mass object with $T_{\rm eff} = 2500$ K.
4. Based on literature and this survey, we identify a sample of 21 spectroscopically confirmed young BD members within our survey area of ρ Oph. However, this sample, based on current existing surveys, is likely highly incomplete, due to the variable and high extinction in ρ Oph.
5. From MOIRCS, 2MASS, and *Spitzer* photometry, a sample of 27 sources with mid-infrared color excess and near-infrared colors indicative for substellar mass sources with disks are identified. Of these, 11 are previously spectroscopically confirmed BDs, while 16 are newly identified candidates.
6. Based on present-day surveys of the stellar and BD populations, the ratio of substellar to stellar sources in ρ Oph is derived to have an upper limit of 5–7. This is in line with other nearby young star-forming regions.

The authors thank Kentaro Aoki for supporting the spectroscopy run with Subaru/MOIRCS, Laura Fissel for discussion on the image reduction, and an anonymous referee for useful suggestions for improving the paper. A.S. acknowledges financial support through the UK/PATT grant SPA0-YST003 and the grant 10/RFP/AST2780 from the Science Foundation Ireland. R.J. acknowledges support from NSERC grants as well as a Royal Netherlands Academy of Arts and Sciences (KNAW) visiting professorship. This publication makes use of data products from the Two Micron All Sky Survey, which is a joint project of the University of Massachusetts and the Infrared Processing and Analysis Center/California Institute of Technology, funded by the National Aeronautics and Space Administration and the National Science Foundation. This research makes use of the SIMBAD database, operated at CDS, Strasbourg, France.

REFERENCES

Allard, F., Hauschildt, P. H., Alexander, D. R., Tamanai, A., & Schweitzer, A. 2001, ApJ, 556, 357
Allen, L. E., et al. 2004, ApJS, 154, 363
Allers, K. N., et al. 2007, ApJ, 657, 511
Alves de Oliveira, C., & Casali, M. 2008, A&A, 485, 155
Alves de Oliveira, C., Moraux, E., Bouvier, J., Bouy, H., Marmo, C., & Albert, L. 2010, A&A, 515, A75
Andersen, M., Meyer, M. R., Greissl, J., & Aversa, A. 2008, ApJ, 683, L183
Baraffe, I., Chabrier, G., Barman, T. S., Allard, F., & Hauschildt, P. H. 2003, A&A, 402, 701
Barsony, M., Kenyon, S. J., Lada, E. A., & Teuben, P. J. 1997, ApJS, 112, 109
Bertin, E., & Arnouts, S. 1996, A&AS, 117, 393
Bessell, M. S., & Brett, J. M. 1988, PASP, 100, 1134
Bonnell, I. A., Larson, R. B., & Zinnecker, H. 2007, in Protostars and Planets V, ed. B. Reipurth, D. Jewitt, & K. Keil (Tucson, AZ: Univ. Arizona Press), 149
Bontemps, S., et al. 2001, A&A, 372, 173
Caballero, J. A., et al. 2007, A&A, 470, 903
Comeron, F., Rieke, G. H., Burrows, A., & Rieke, M. J. 1993, ApJ, 416, 185
Cushing, M. C., Rayner, J. T., & Vacca, W. D. 2005, ApJ, 623, 1115
Cushing, M. C., Tokunaga, A. T., & Kobayashi, N. 2000, AJ, 119, 3019
Cutri, R. M., et al. 2003, 2MASS All Sky Catalog of Point Sources, The IRSA 2MASS All-Sky Point Source Catalog, NASA/IPAC Infrared Science Archive, http://irsa.ipac.caltech.edu/applications/Gator/
de Geus, E. J., de Zeeuw, P. T., & Lub, J. 1989, A&A, 216, 44
Greene, T. P., & Young, E. T. 1992, ApJ, 395, 516
Jayawardhana, R., Ardila, D. R., Stelzer, B., & Haisch, K. E. 2003, AJ, 126, 1515
Jayawardhana, R., & Ivanov, V. D. 2006, ApJ, 647, L167
Jayawardhana, R., Mohanty, S., & Basri, G. 2002, ApJ, 578, L141
Jordi, K., Grebel, E. K., & Ammon, K. 2006, A&A, 460, 339
Kirkpatrick, J. D., Barman, T. S., Burgasser, A. J., McGovern, M. R., McLean, I. S., Tinney, C. G., & Lowrance, P. J. 2006, ApJ, 639, 1120
Lodieu, N., Hambly, N. C., & Jameson, R. F. 2006, MNRAS, 373, 95
Loren, R. B., Wootten, A., & Wilking, B. A. 1990, ApJ, 365, 269
Luhman, K. L., Liebert, J., & Rieke, G. H. 1997, ApJ, 489, L165
Luhman, K. L., & Rieke, G. H. 1999, ApJ, 525, 440
Luhman, K. L., Stauffer, J. R., Muench, A. A., Rieke, G. H., Lada, E. A., Bouvier, J., & Lada, C. J. 2003, ApJ, 593, 1093
Marsh, K. A., Kirkpatrick, J. D., & Plavchan, P. 2010, ApJ, 709, L158
Mathis, J. S. 1990, ARA&A, 28, 37
Meyer, M. R., Calvet, N., & Hillenbrand, L. A. 1997, AJ, 114, 288
Miyazaki, S., et al. 2002, PASJ, 54, 833
Natta, A., Testi, L., Comerón, F., Oliva, E., D'Antona, F., Baffa, C., Comoretto, G., & Gennari, S. 2002, A&A, 393, 597
Natta, A., Testi, L., & Randich, S. 2006, A&A, 452, 245
Ouchi, M., et al. 2004, ApJ, 611, 660
Pickles, A. J. 1998, PASP, 110, 863
Ratzka, T., Köhler, R., & Leinert, C. 2005, A&A, 437, 611
Ridge, N. A., et al. 2006, AJ, 131, 2921
Scholz, A., Geers, V., Jayawardhana, R., Fissel, L., Lee, E., Lafreniere, D., & Tamura, M. 2009, ApJ, 702, 805
Skrutskie, M. F., et al. 2006, AJ, 131, 1163
Smith, J. A., et al. 2002, AJ, 123, 2121
Suzuki, R., et al. 2008, PASJ, 60, 1347
Wilking, B. A., Gagné, M., & Allen, L. E. 2008, in ASP Monograph Publications, Star Formation in the ρ Ophiuchi Molecular Cloud, ed. B. Reipurth (San Francisco, CA: ASP), 351
Wilking, B. A., Greene, T. P., & Meyer, M. R. 1999, AJ, 117, 469
Wilking, B. A., & Lada, C. J. 1983, ApJ, 274, 698
Wilking, B. A., Meyer, M. R., Robinson, J. G., & Greene, T. P. 2005, AJ, 130, 1733
Witte, S., Helling, C., & Hauschildt, P. H. 2009, A&A, 506, 1367
Yagi, M., Kashikawa, N., Sekiguchi, M., Doi, M., Yasuda, N., Shimasaku, K., & Okamura, S. 2002, AJ, 123, 66